ORGANOMETALLICS

Article

Cite This: *Organometallics* XXXX, XXX, XXX−XXX

pubs.acs.org/Organometallics

Selective Ethylene Dimerization by Palladium(II) Complexes Bearing a Phosphinoferrocene Sulfonate Ligand

Martin Zábranský,[†] Werner Oberhauser,*[,‡] Gabriele Manca,[‡] Ivana Císařová,[†] and Petr Štěpnička*[,†]

[†]Department of Inorganic Chemistry, Faculty of Science, Charles University, Hlavova 2030, 128 40 Prague, Czech Republic

[‡]Istituto di Chimica dei Composti Organometallici, Consiglio Nazionale delle Ricerche (ICCOM-CNR), Via Madonna del Piano 10, 50019 Sesto Fiorentino, Italy

Supporting Information

ABSTRACT: Palladium(II) complexes featuring the hybrid anionic ligand 1′-(diphenylphosphino)ferrocene-1-sulfonate ($\mathbf{L}^-$), viz., *trans*-$(Et_3NH)_2[Pd(\mu\text{-}Cl)Me(\mathbf{L}\text{-}\kappa P)]_2$ (**1**), $[Pd(Me)(dmap\text{-}\kappa N^1)(\mathbf{L}\text{-}\kappa^2 O,P)]$(**2**; dmap = 4-(dimethylamino)pyridine), and $[Pd(\eta^3\text{-allyl})(\mathbf{L}\text{-}\kappa^2 O,P)]$ (**6**), were synthesized and together with the previously reported compounds *trans*-$(Et_3NH)_2[PdCl_2(\mathbf{L}\text{-}\kappa P)_2]$ and $[Pd(L^{CY})(\mathbf{L}\text{-}\kappa^2 O,P)]$ (L^{CY} = 2-[(dimethylamino-κ*N*)methyl]phenyl-κC^1 and 2-[(methylthio-κ*S*)methyl]phenyl-κC^1) tested as precatalysts for Pd-catalyzed ethylene dimerization. Only compound **1** gave rise to an active catalyst after activation by sequential halogen removal with $Tl[PF_6]$ and $Na[BAr'_4]$ (Ar′ = 3,5-bis(trifluoromethyl)phenyl) in chloroform. Thus, the formed catalyst efficiently mediated the dimerization of ethylene showing both good activity (TOF ≈ 95 h^{-1}) and high selectivity for 1-butene (95%) at 21 °C and 30 bar of ethylene pressure. DFT calculations have shown that the dimerization reaction is thermodynamically preferred over the formation of higher oligomers and that *O*,*P*-chelate coordination of the phosphinosulfonate ligand in all Pd(II) reaction intermediates is vital for the catalytic process. In particular, the *O*,*P*-chelating phosphinoferrocene sulfonate ligand stabilizes and electronically differentiates the reaction intermediates and favors concerted ethyl migration to coordinated ethylene giving rise to 1-butene.

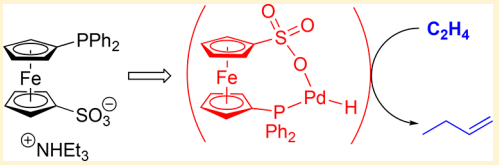

INTRODUCTION

Alkylpalladium(II) complexes bearing auxiliary *ortho*-(phosphino)arenesulfonate ligands (**A** in Scheme 1) show unique properties in ethylene copolymerization with various polar vinyl monomers, preferentially producing linear functionalized polymers.[1,2] In ethylene homopolymerization, these complexes produce polyethylene with high molecular weight (typically in the 10^3−10^5 range) and linearity (1−10 branches per 1000 carbon atoms).[1b] Theoretical[3] and experimental[4] studies performed on Pd(II) complexes with *O*,*P*-coordinated phosphinosulfonate ligands have shown that the high linearity of the polymeric product results from the anionic nature of the *O*,*P* ligand, which reduces the positive charge at the metal center, thereby suppressing *β*-hydride elimination in the presence of ethylene monomer.[1]

Scheme 1. Relevant Examples of Phoshinosulfonate Ligands

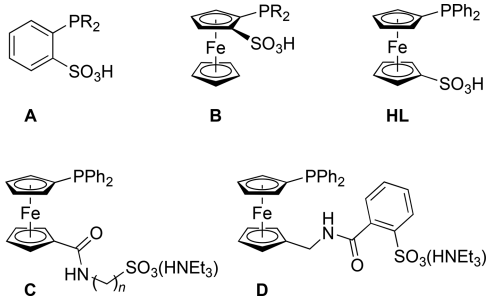

In 2011, Erker et al. synthesized a family of phosphinosulfonate ligands derived from ferrocene (**B**), with the functional groups located in adjacent positions of the same cyclopentadienyl ring.[5] Pd(II) complexes with this ligand coordinated in an *O*,*P*-chelating anionic form yielded ethylene homopolymers with an average molecular weight of 5860 g mol^{-1}.[6] Lower molecular weight polyolefins were detected after oxidation of the iron center by cobaltocene (redox-controlled polymerization).[6b] This finding is consistent with the electron-withdrawing nature of the ferrocenium moiety[7] and with its role in promoting chain transfer via *β*-hydride elimination.

Continuing our research focused on hydrophilic, ferrocene-based phosphinosulfonate ligands that has led to the preparation of compounds **C**[8] and **D**[9] (Scheme 1), we have recently reported the synthesis of 1′-(diphenylphosphino)-ferrocene-1-sulfonic acid (**HL** in Scheme 1). This compound is a sterically distinct isomer of **B**-type ligands and can be conveniently isolated in the form of the stable salt (Et_3NH)**L**.[10] Considering the attractive catalytic behavior of phosphinosulfonate ligands in polymerization reactions, we extended our studies with **HL**[10,11] toward the synthesis of Pd(II) complexes with selected hydrocarbyl ligands and toward

Received: January 14, 2019

DOI: 10.1021/acs.organomet.9b00015
Organometallics XXXX, XXX, XXX−XXX

Scheme 2. Synthesis and Reactivity of Methylpalladium(II) Complexes[a]

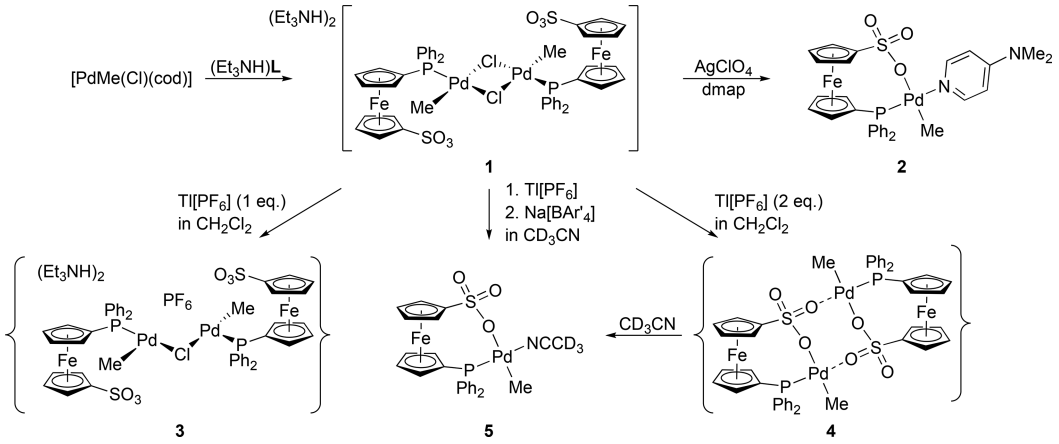

[a]Legend: cod = cycloocta-1,5-diene, dmap = 4-(dimethylamino)pyridine, Na[BAr′$_4$] = sodium tetrakis[3,5-bis(trifluoromethyl)phenyl]borate

application of these compounds in selective ethylene dimerization to 1-butene under homogeneous reaction conditions.

Ethylene dimerization to 1-butene, which is the widely used comonomer in the synthesis of low-density polyethylene, is industrially performed using the AlphaButol process and a Ti-based catalyst.[12] The latter is highly selective toward 1-butene thanks to the coupling of two ethylene molecules, which form a metallacyclopentane intermediate during the reaction.[13] Late-transition metal complexes featuring neutral[14] and anionic[15] chelating ligands do not generally show good selectivity in the dimerization of ethylene to 1-butene mostly because of their high isomerization activity. However, high 1-butene selectivity (>98%) was achieved when using Ni(II)[16] and Co(II)[17] precatalysts stabilized by tridentate ligands and activated through alkylation with alkylaluminum reagents. In this contribution, we report our results from selective ethylene dimerization to 1-butene using Pd(II)-**L** precatalysts, from the structural characterization of these compounds and, also, from a DFT study, which enabled us to propose an operative catalytic cycle of the selective 1-butene production.

RESULTS AND DISCUSSION

Synthesis and Characterization of the Precatalysts. For catalytic testing, we prepared Pd(II) complexes bearing hydrocarbyl ligands capable of inserting ethylene, either directly (methyl) or after a haptotropic isomerization (allyl), and relatively weaker binding ligands (sulfonate oxygen, solvent or an N-donor). The starting material for the preparation of the methylpalladium(II) complexes was dipalladium complex *trans*-(Et$_3$NH)$_2$[Pd(*μ*-Cl)(Me)(**L**-*κP*)]$_2$ (**1** in Scheme 2), obtained by replacing coordinated 1,5-cyclooctadiene (cod) in [PdMe(Cl)(cod)] with 1 equiv of (Et$_3$NH)**L**. The formation of this complex, rather than a monopalladium(II) chelate such as [PdMe(Cl)(**L**-*κ*^{2}*O*,*P*)], corresponds with the preference of Pd(II) for coordinating soft donors.[18] A similar reaction using 2 equiv of (Et$_3$NH)**L** produced a different species, which was converted into bis(phosphine) complex *trans*-(Et$_3$NH)$_2$[PdCl$_2$(**L**-*κP*)$_2$][10] upon recrystallization from a halogenated solvent and therefore was not further investigated.

NMR signals due to PdMe in complex **1** are found at δ_H 0.73 (d, $^3J_{PH}$ = 2.2 Hz) and δ_C 6.27 (br s), thus corroborating the *cis*-P,C relationship. The ^{1}H and ^{13}C NMR spectra further display signals of the Et$_3$NH$^+$ cations and of the ferrocene ligand (including the characteristic, low-field signal due to C–SO$_3$ at δ_C 94.57). ^{31}P NMR resonance of **1** occurs as a singlet at δ_P 31.3.

Compound **1** is reluctant to crystallize, typically separating as a viscous, orange oil. However, when using a wet mixed solvent (see the Experimental Section), compound **1** was converted into the better crystallizing monohydrate **1**·H$_2$O, which was structurally authenticated by X-ray diffraction analysis (Figure 1). Atoms forming the central {Pd(*μ*-Cl)P(C)}$_2$ moiety in the structure of **1**·H$_2$O are coplanar within 0.2 Å. An inspection of Pd-donor distances and interligand angles (Table 1) reveals a minor asymmetry in the Pd–Cl bonds and an opening of the *cis*-P–Pd–Cl angles compensated for by the small in-ring Cl1–Pd–Cl2 angles.[19] The ferrocene units, located on the same side with respect to the coordination plane, are tilted by approximately 4° and assume different conformations, as shown by the torsion angle C1–Cg1–Cg2–C6 (*τ*), where Cg1 and Cg2 are the centroids of the cyclopentadienyl rings C(1–5) and C(6–10), respectively, *τ* = −88.1(5)° (Fe1), and −155.4(5)° (Fe2). The different mutual orientations of the substituents at the ferrocene units reflect steric interactions (**L**$^-$ is the bulkiest

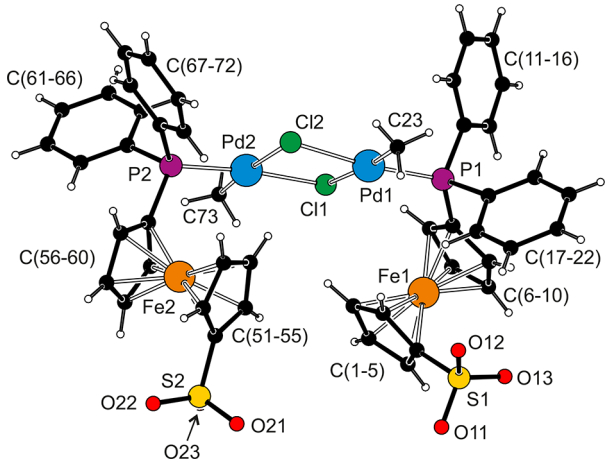

Figure 1. View of the complex anion in the structure of **1**·H$_2$O (for complete displacement ellipsoid plot, see the Supporting Information).

DOI: 10.1021/acs.organomet.9b00015
Organometallics XXXX, XXX, XXX–XXX

Table 1. Selected Distances and Angles (in Å and deg) for Compound 1·H_2O

Pd1−P1	2.223(2)	Pd2−P2	2.214(2)
Pd1−Cl1	2.446(1)	Pd2−Cl1	2.412(1)
Pd1−Cl2	2.414(1)	Pd2−Cl2	2.475(1)
Pd1−C23	2.037(7)	Pd2−C73	2.053(7)
P1−Pd1−Cl1	98.68(5)	P2−Pd2−Cl2	102.51(5)
P1−Pd1−C23	87.7(2)	P2−Pd2−C73	85.7(2)
Cl1−Pd1−Cl2	83.57(5)	Cl1−Pd2−Cl2	82.99(5)
Cl2−Pd1−C23	89.9(2)	Cl1−Pd1−C73	88.9(2)

ligand in the coordination sphere) and are certainly affected by hydrogen-bonding interactions of the ligands' sulfonate groups with the counterions and the water molecules (see the Supporting Information).

Removing the chloride ligands from **1** with $AgClO_4$ in the presence of 4-(dimethylamino)pyridine (dmap) affords compound **2**, which results from the elimination of AgCl and $(Et_3NH)ClO_4$. The complex containing *O,P*-chelating phosphinosulfonate $\mathbf{L}^-$ was also structurally characterized. Notably, pyridine reacts similarly but has to be used in a large excess (as the solvent). In addition, the product easily decomposes and is therefore unsuitable for further studies.

The NMR spectra of **2** display signals due to PdMe (δ_H 0.27 and δ_C 1.75; both split into doublets) and the dmap ligand (but not the characteristic resonances of the Et_3NH^+ cations). The ^{31}P NMR signal of **2** (δ_P 29.9) appears slightly shifted to a higher field than that of the parent complex **1**. Notably, both **1** and **2** give rise to ions $[PdMe(\mathbf{L}) + H]^+$ (*m/z* 571), which are the heaviest fragments in their ESI+ mass spectra.

Compound **2** crystallized in a solvated form (**2**·1/2AcOEt) with the solvent molecules extensively disordered within the structural voids. The molecular structure (Figure 2) corroborates the *trans*-P,N arrangement in which the donors with the strongest *trans* influence[20] (Me and PR_3) occupy adjacent (*cis*) positions.[21] The palladium and its four ligating atoms lie in a plane (within ≈0.08 Å), yet the coordination environment is somewhat twisted due to different Pd-donor distances, unlike

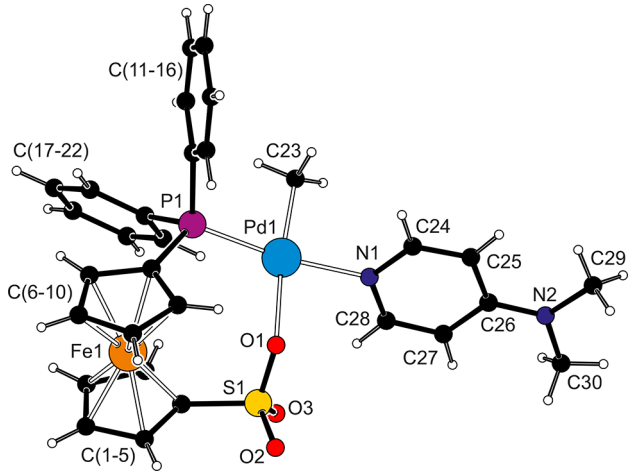

Figure 2. View of the complex molecule in the structure of **2**·1/2AcOEt. Selected distances and angles (in Å and deg): Pd1−P1 2.2488(6), Pd1−O1 2.167(2), Pd1−N1 2.104(2), Pd1−C23 2.026(2), P1−Pd1−O1 100.26(5), P1−Pd1−C23 86.21(7), C23−Pd1−N1 87.66(8), N1−Pd1−O1 86.00(7). The displacement ellipsoid plot is provided in Supporting Information.

spatial demands of the ligands and the chelating coordination of the phosphinoferrocene sulfonate anion, which results in the most opened interligand angle (≈100°). In fact, the bite angle of the phosphinoferrocene ligand is larger (by ≈5−6°) than that of the 2-(diphenylphosphino)benzenesulfonate ligand in the structure of $[Pd(Me)(py)(2\text{-}Ph_2PC_6H_4SO_3\text{-}\kappa^2O,P)]$ (py = pyridine).[22] The pyridine ligand in **2** binds Pd1 at the distance of 2.104(2) Å and is rotated by 62.63(9)° from the coordination plane, {Pd1, P1, O1, N1, C23}. Last, the ferrocene cyclopentadienyls are tilted by 2.1(1)° and adopt a closed (approximately 1,2′ or synperiplanar eclipsed)[23] conformation characterized by the τ angle of 61.8(2)°, which is consistent with the *O,P*-chelate coordination of the ligand $\mathbf{L}^-$.

When treated with $Tl[PF_6]$ (1 equiv) in CH_2Cl_2, **1** produces intermediate **3** in an 80% yield (Scheme 2). The $^{31}P\{^1H\}$ NMR spectrum of **3** showed a singlet at δ_P 30.7. Signals of the Pd-bound methyl group were observed at δ_H 0.75 (s) and at δ_C 6.22 (br s), suggesting that the *cis* arrangement of the methyl and phosphine ligands was retained. The ^1H NMR ferrocene signals and the IR spectrum (KBr) of **3** are very similar to those of **1**. Hence, we deduce that **3** likely has a dimeric structure featuring one chloride bridge between two equivalent Pd(II) metal centers with a T-shaped coordination geometry.[24]

An analogous reaction between **1** and 2 equiv of $Tl[PF_6]$ in CH_2Cl_2, followed by removing $(Et_3NH)[PF_6]$ from the reaction mixture by extraction with water led, to the formation of a yellow compound **4** that was completely insoluble in noncoordinating organic solvents such as $CHCl_3$. The IR spectrum of this material attested to the presence of coordinated $-SO_3^-$ units, presumably in a dimeric compound containing a symmetrical $(Pd-O)_2$ core.[6b] CD_3CN addition dissolved **4**, thereby forming neutral monomeric species **5**, which was characterized *in situ* by NMR spectroscopy. The same compound was obtained when **1** was treated successively with $Tl[PF_6]$ and $Na[BAr'_4]$ (Ar′ = 3,5-bis(trifluoromethyl)-phenyl) in CD_3CN.

Even in this case, the NMR spectra suggested that the methyl and phosphine moieties occupy *cis* positions [PdMe: δ_H 0.35 (s), δ_C −1.73 (d, $^2J_{PC}$ = 4 Hz)]. The ferrocene protons of **5** gave rise to four signals at δ_H 4.13, 4.42, 4.61 and 4.71, and the IR spectra indicated the presence of a coordinated SO_3^- unit.[25]

In addition to the PdMe complexes, we have also synthesized Pd(η^3-allyl) complex **6** (Scheme 3). The

Scheme 3. Synthesis of (η^3-Allyl)Pd(II) Complex 6

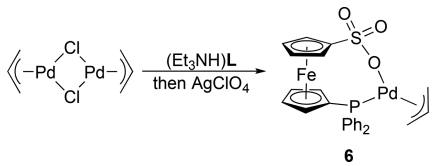

6

compound was prepared in good yield (≈80%) by $[Pd(\mu\text{-}Cl)(\eta^3\text{-}C_3H_5)]_2$ cleavage with a stoichiometric amount of $(Et_3NH)\mathbf{L}$ and subsequent $AgClO_4$ addition, resulting in the elimination of AgCl and $(Et_3NH)ClO_4$.

The NMR spectra of **6** confirm the formulation by showing only the signals due to the phosphinoferrocene ligand and to the η^3-bound allyl moiety. ^1H NMR signals of the allyl CH_2 group *trans* to the oxygen donor are observed as broad singlets at very similar positions, whereas those due to the methylene

DOI: 10.1021/acs.organomet.9b00015
Organometallics XXXX, XXX, XXX−XXX

group *trans* to the phosphine moiety give rise to well-resolved and markedly anisochronic multiplets ($\Delta\delta_H \approx 1$ ppm). The corresponding ^{13}C NMR signals are observed at δ_C 53.55 (d, $^2J_{PC}$ = 2 Hz, CH_2 *trans*-O) and 85.77 (d, $^2J_{PC}$ = 27 Hz, CH_2 *trans*-P), following the trend in *trans*-influence. The signals due to the meso CH group occur at δ_H 5.78 (m) and at δ_C 120.01 (d, $^2J_{PC}$ = 5 Hz).

Structure determination of complex **6** revealed a pseudo-trigonal coordination environment around the Pd(II) center (Figure 3 and Table 2). The η^3-allyl moiety is characteristically

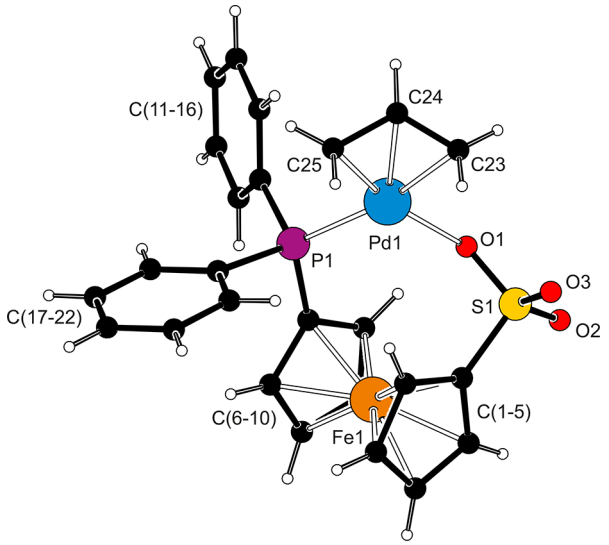

Figure 3. View of the molecular structure of **6** (conventional displacement ellipsoid plot is provided in Supporting Information).

Table 2. Selected Distances and Angles (in Å and deg) for Complex 6[a]

Pd1−P1	2.2990(6)	P1−Pd1−O1	97.29(3)
Pd1−O1	2.123(1)	C23−C24−C25	118.8(2)
Pd1−C23	2.187(2)	C23−Pd1−C25	68.06(7)
Pd1−C24	2.138(2)	∠Cp1,Cp2	1.3(1)
Pd1−C25	2.100(2)	τ	−61.3(1)

[a]Cp1 and Cp2 are the cyclopentadienyl rings C(1−5) and C(6−10), respectively. Cg1 and Cg2 denote their respective centroids. τ is the torsion angle C1−Cg1−Cg2−C6.

tilted[26] (by 68.4(2)°) from the plane defined by the palladium and the remaining donor atoms, {Pd1, P1, O1}, and coordinates rather symmetrically with respect to the other donors (cf. P1−Pd1−C25 = 98.40(6)° and O1−Pd1−C23 = 96.26(6)°). Notably, the Pd−C distances decrease gradually from C23 to C25,[27] reflecting the relatively larger *trans* influence[20] of the phosphine donor. The ferrocene unit in the *O,P*-chelating ligand adopts an approximate 1,2′ conformation, similar to that encountered in **2**·1/2AcOEt.

Catalytic Experiments. Compounds **1**−**4**, **6**, *trans*-$(Et_3NH)_2[PdCl_2(\mathbf{L}\text{-}\kappa P)_2]$,[10] and the complexes with the *ortho*-metalated ligands, $[(L^{CY})Pd(L\text{-}\kappa^2 O,P)]$ (L^{CY} = 2-[(dimethylamino-κN)methyl]phenyl-κC^1 or 2-[(methylthio-κS)methyl]phenyl-κC^1),[10] were initially screened in the ethylene oligomerization reaction in the absence of any additional activators. The testing reactions were conducted in chloroform at 21 °C in the presence of 30 bar of ethylene. Under such conditions, however, none of the compounds was catalytically active, which is presumably due to strong coordination of the coligands: dmap in **2**, chloride in **1** and **2**, or L^{CY} in the *ortho*-metalated compounds. Complex **5** was stable only in the presence of acetonitrile, whereas a $\eta^3 \rightarrow \eta^1$ haptotropic change of the allyl unit in **6**, necessary for the ethylene coordination to Pd(II), would be associated with a high energy cost.

Next, we activated precatalyst **3** *in situ* with an excess of $Na[BAr'_4]$ (2.0 equiv) in chloroform saturated with ethylene. ^1H NMR spectra acquired during the reaction of the formed species with ethylene (at room temperature in $CDCl_3$) are presented in Figure 4. The ^1H NMR traces b−d clearly show

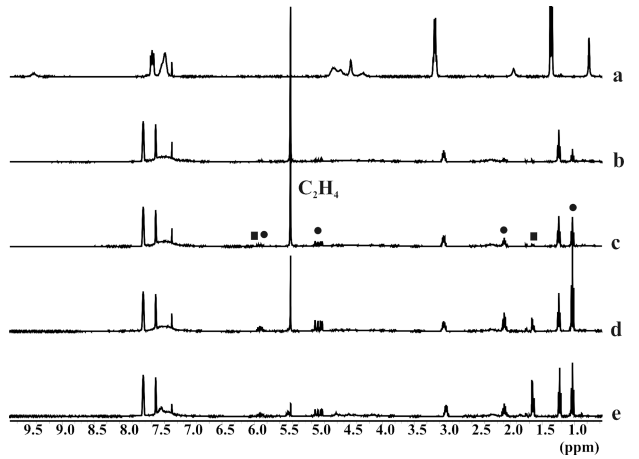

Figure 4. ^1H NMR spectra (400 MHz, $CDCl_3$, 21 °C) recorded during the **3**/$Na[BAr'_4]$-mediated ethylene dimerization reaction: (a) precursor **3**; (b) spectrum obtained after saturation with ethylene and addition of $Na[BAr'_4]$; and spectra taken after (c) 15 min, (d) 1 h, and (e) 2 h of reaction time (● = 1-butene, ■ = *cis*,*trans*-2-butene).

the conversion of ethylene into 1-butene during the reaction. Once the concentration of dissolved ethylene decreased (trace e), however, 1-butene was isomerized to *trans*/*cis*-2-butene (2:1 ratio) by the same catalyst (additional ^1H NMR spectra of the reaction mixtures and *operando* ^{31}P NMR spectra are available as the Supporting Information). An analogous control ^1H NMR experiment performed in the presence of pyridine (pyridine/**3** molar ratio = 2), which coordinates Pd(II) (albeit less strongly than dmap), indicated that no ethylene dimerization occurred.

In order to validate the catalytic system in terms of selectivity and catalyst stability, we conducted additional catalytic reactions with **3**/$Na[BAr'_4]$ in $CDCl_3$ under different ethylene pressures and reaction times (Table 3).

The highest 1-butene selectivity (95%) was attained when the catalytic reactions were performed at 21 °C in the presence of 30 bar of ethylene for 1 h (TOF = 95 h^{-1}; Table 3, entry 3). Prolonging the reaction time to 3, 6, and 12 h under such conditions led to a gradual though only slight decrease of the selectivity (down to 89%, entries 3−5), otherwise corroborating the stability of the catalyst under the specified reaction conditions. The lower TOF value achieved at a shorter reaction time (0.5 h; Table 3, entry 1) suggests the presence of an induction period due to the conversion of **3** into the true catalytically active species. Indeed, GC-MS analysis of the reaction mixtures revealed trace amounts of propene, which stems from the conversion of the starting Pd−Me species into the catalytically active Pd−H species (i.e., catalytic activation

DOI: 10.1021/acs.organomet.9b00015
Organometallics XXXX, XXX, XXX−XXX

Table 3. Summary of the Catalytic Results[a]

		selectivity (%)[b]			
entry	t (h)	1-C_4	2-C_4	1-C_6	TOF (h^{-1})[c]
1	0.5	94	5	trace	85
2	1	95	4	1	95
3	3	92	7	1	94
4	6	91	8	1	93
5	12	89	10	1	91
6[d]	1	81	18	1	283
7[e]	1	58	40	2	415
8[e]	3	57	41	2	180
9[f]	1	92	8	trace	83

[a]Conditions: **3** (14.0 mg, 9.0 μmol), Na[BAr′$_4$] (16.0 mg, 18.1 μmol), $CDCl_3$ (4.0 mL), $p(C_2H_4)$ = 30.0 bar, T = 21 °C. The autoclave was cooled to −20 °C before unreacted ethylene was released and the products analyzed by ^{1}H NMR spectroscopy. [b]Selectivity to 1-butene (1-C_4)l sum of *cis*/*trans*-2-butenes (2-C_4) and 1-hexene (1-C_6) was determined by ^{1}H NMR integration. [c]TOF was determined by ^{1}H NMR using toluene as a standard. [d]Reaction at 35 °C. [e]Reaction at 50 °C. [f]$p(C_2H_4)$ = 5.0 bar.

by insertion of ethylene into the Pd−Me bond followed by β-elimination).

At a lower ethylene pressure (5.0 bar), the selectivity to 1-butene remained nearly unchanged (92%) but the yield of the dimerization product was decreased (TOF of 83 h^{-1}; entry 9). Conversely, increasing the reaction temperature to 35 and 50 °C accelerated both the dimerization reaction and the subsequent 1-butene isomerization to 2-butenes. Consequently, the selectivity toward 1-butene gradually decreased from 95% (21 °C) to 81% (35 °C) and 58% (50 °C; Table 3, entries 2, 6, and 7). In addition, palladium black formation was observed at 50 °C, which corresponds with the observed decrease in the catalytic activity noted at the this temperature after 3 h of the reaction time (Table 3, entries 8 and 7). Notably, only small amounts of the trimerization product, 1-hexene (<2%), could be detected in all experiments.

To experimentally prove the role of the sulfonate moiety during the catalytic process, we used a related complex *trans*-[Pd(μ-Cl)(Me)(PPh_2Fc)]$_2$ (**7**)[28] (see the Supporting Information) bearing an analogous ferrocene-based ligand without the sulfonate unit. When utilizing this precatalyst and applying the standard reaction conditions, a complete decomposition of the reaction mixture was observed. In addition, the ^{1}H NMR spectrum proved that no 1-butene was formed. An additional *operando* NMR experiment with **7** was carried out in the presence of hexadecyltrimethylammonium *p*-toluensulfonate, ethylene, and Na[BAr′$_4$], showing again no 1-butene formation. Instead, a gradual decomposition of activated **7** took place. We thus infer that chelating coordination of $\mathbf{L}^-$ anion to Pd(II) plays a crucial role in stabilizing the metal center during the catalytic reaction. This experimental result is in agreement with DFT computations, which revealed that the *O*,*P*-chelating coordination of the anionic ligand $\mathbf{L}^-$ to a PdMe(η^2-C_2H_4) fragment is 13.3 kcal mol^{-1} more stable than the isomeric trigonal species featuring P-monodentate ligand. The entire catalytic cycle, elucidated by DFT calculations, is presented in Scheme 4.

Precatalyst **3** enters the catalytic cycle via activation with Na[BAr′$_4$] (elimination of Pd-bound chloride) and elimination of propene formed by ethylene insertion into the Pd-Me bond and subsequent β-hydride elimination. The resulting tricoordinate Pd−H species (**A**), with hydride positioned *cis* to the phosphine donor moiety, coordinates ethylene to produce **B**, which in turn undergoes ethylene insertion, producing another tricoordinate intermediate, **C**. The latter may react in two ways: either continues the productive catalytic cycle 1 or enters into catalytic cycle 2, which produces 1-hexene (Scheme 4). Nonetheless, exoergic isomerization of **C** followed by ethylene coordination, which yields intermediate **E**, is favored over ethylene coordination to the former species (cf. −37.9 kcal mol^{-1} *vs* −22.7 kcal mol^{-1}). This finding is confirmed by the low amount of 1-hexene found in the reaction mixture. The migration of the coordinated ethyl unit in **E** and concomitant M−H bond formation leads to the transition state $\mathbf{F}^{TS}$ (concerted reaction mechanism), which is associated with an overall energy gain of 2.5 kcal mol^{-1}. Figure 5 shows the computed structure for $\mathbf{F}^{TS}$. The release of the main product (1-butene) is associated with an energy cost of 8.5 kcal mol^{-1}, regenerating Pd−H species **A**.

Ethylene coordination to intermediate **C** gives rise to alkene-alkyl species **G**, which undergoes ethylene insertion. Resulting intermediate **H** is characterized by an agostic Pd−H interaction (Figure 5; the isomeric species with the *n*-butyl group *trans* to the phosphorus atom could not be optimized). Ethylene coordination to the intermediate **H** and its insertion

Scheme 4. Plausible Catalytic Cycle for Ethylene Dimerization Based on DFT Calculations[a]

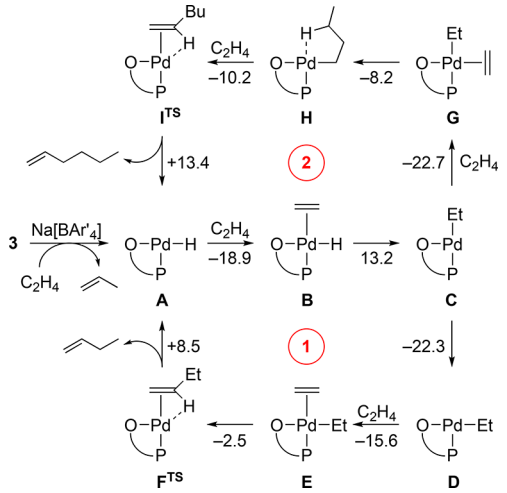

[a]P∼O = 1′-(diphenylphosphino)ferrocene-1-sulfonate ($\mathbf{L}^-$), Na[BAr′$_4$] = sodium tetrakis[3,5-bis(trifluoromethyl)phenyl]borate, TS = transition state. Energies are given in kcal mol^{-1}.

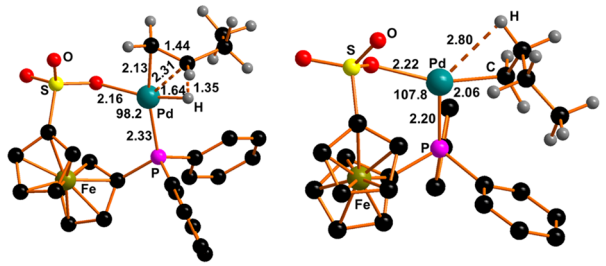

Figure 5. DFT-optimized structures of $\mathbf{F}^{TS}$ (left) and **H** (right) and relevant interatomic distances (in Å) and angles (in deg). Hydrogen atoms have been omitted for clarity, except those of the hydrocarbyl group bounded to Pd.

DOI: 10.1021/acs.organomet.9b00015
Organometallics XXXX, XXX, XXX−XXX

lead to the transition state $\mathbf{I}^{TS}$, which resembles $\mathbf{F}^{TS}$. Overall, catalytic cycle 2 is approximately 5.0 kcal mol^{-1} less exoergic than cycle 1.

CONCLUSIONS

A series of Pd(II) complexes combining Pd-bound hydrocarbyl ligands and 1′-(diphenylphosphino)ferrocene-1-sulfonate ligand in their structure has been synthesized. Of all compounds tested in this study, only coordinatively unsaturated (preactivated) intermediate **3** could be converted into an active catalyst for selective ethylene dimerization into 1-butene by Na[BAr′$_4$] addition. The catalytic activity of such catalyst, presumably structurally analogous to complex **5**, remained stable over time (TOF = 95 h^{-1}) and showed selectivity toward 1-butene up to 95%, when the reactions are carried out at 21 °C and under high ethylene pressure (30 bar). Notably, the behavior of Pd−L complexes markedly contrasts with that of the analogous complexes bearing the isomeric 2-phosphinoferrocenesulfonate ligands (**B** in Scheme 1) that typically convert ethylene into higher oligomers or even into high molecular weight polyethylene.

DFT calculations confirmed our experimental observations, showing that the stability of the catalyst is mainly due to *O,P*-chelating coordination to Pd(II) of the ferrocene phosphinosulfonate ligand $\mathbf{L}^-$ in all involved intermediates. In addition, they indicated that 1-butene is selectively formed thanks to a concerted ethyl migration to coordinated ethylene (the ethyl group in the intermediate is located *trans* to the coordinating sulfonate oxygen atom) and subsequent *β*-hydride elimination. Finally, the computations suggested that the formation of 1-butene is thermodynamically favored over that of higher oligomers (e.g., 1-hexene).

EXPERIMENTAL SECTION

General Considerations. (Et$_3$NH)**L**,[10] [PdCl(Me)(cod)],[29] and sodium tetrakis[3,5-bis(trifluoromethyl)phenyl]borate (Na[BAr′$_4$])[30] were synthesized using methods previously reported in the literature. Ethylene (99.95%) used for catalytic tests was purchased from GHC Gerling, Holz & Co., and Aldrich, respectively. Other chemicals were purchased from commercial supplies (Sigma-Aldrich or Alfa-Aesar) and were used as received. $CDCl_3$ (Signa-Aldrich) was used without further purification. Anhydrous dichloromethane used for syntheses was obtained using a PureSolv MD5 solvent purification system (Innovative Technology, Inc., Amesbury, MA, USA).

^{1}H, ^{31}P{^{1}H}, and ^{13}C{^{1}H} NMR spectra were recorded with a Varian Unity Inova 400 or a Bruker AVANCE 400 spectrometer (^{1}H, 400 MHz; ^{31}P, 162 MHz; and ^{13}C, 101 MHz) at 20 or 25 °C. Chemical shifts (δ in ppm) are expressed relative to internal tetramethylsilane (^{1}H and ^{13}C) and to external 85% aqueous H_3PO_4 (^{31}P). In addition to the standard notation of signal multiplicity (s = singlet, d = doublet, t = triplet, etc.),[31] vt and vq are used to denote virtual multiplets arising from the AA′BB′ and AA′BB′X spin systems (A, B = ^{1}H, X = ^{31}P) by the hydrogen atoms at the sulfonate- and phosphine-substituted cyclopentadienyl rings, respectively. IR spectra in KBr pellets were acquired on a PerkinElmer Spectrum BX spectrometer. Electrospray ionization (ESI) mass spectra were recorded on a Compact QTOF-MS spectrometer (Bruker Daltonics). Catalytic reactions were performed in a PTFE-coated, stainless steel autoclave (volume: 70 mL), equipped with a magnetic stirrer and temperature and pressure controllers. GC-MS analyses of the reaction mixtures were performed using a Shimadzu QP2010 GC-MS apparatus with a SPB1 capillary column (30.0 m × 0.25 mm i.d.).

Syntheses. *Synthesis of 1.* A solution of (Et$_3$NH)**L** (220.6 mg, 0.40 mmol) in dichloromethane (5 mL) was added to [PdCl(Me)-(cod)] (106.0 mg, 0.4 mmol) in the same solvent (3 mL). The resulting orange mixture was stirred for 3 h and filtered through a PTFE syringe filter (0.45 μm). The filtrate was successively layered with ethyl acetate/dichloromethane (1:1, 4 mL), a mixture of standard and wet ethyl acetate (1:1, 8 mL), and finally hexane (20 mL). Crystals that formed within a week were filtered off, washed with hexane and pentane, and vacuum-dried over P_2O_5. Yield of **1**·H$_2$O: orange crystalline solid, 268.5 mg (94%). Wet ethyl acetate was obtained by shaking a water−ethyl acetate mixture and by separating the organic solvent. When only such wet ethyl acetate is used for crystallization, as described above, the crystalline product dissolves in water droplets that form upon mixing the solvents. ^{1}H NMR (399.95 MHz, $CDCl_3$): δ 0.73 (d, $^3J_{PH}$ = 2.2 Hz, 3 H, PdMe), 1.34 (t, $^3J_{HH}$ = 7.3 Hz, 9 H, CH_3 of $HNEt_3$), 3.13 (br dq, $^3J_{HH}$ = 7.3 Hz, $^3J_{HH}$ = 4.0 Hz, 6 H, CH_2 of $HNEt_3$), 4.50 (br s, 2 H, fc), 4.61 (br s, 2 H, fc), 4.71 (br s, 2 H, fc), 4.75 (br s, 2 H, fc), 7.31−7.41 (m, 6 H, PPh_2), 7.55−7.61 (m, 4 H, PPh_2), 10.30 (br s, 1 H, *H*NEt_3). ^{31}P{^{1}H} NMR (161.90 MHz, $CDCl_3$): δ 31.3 (s). ^{13}C{^{1}H} NMR (100.58 MHz, $CDCl_3$): δ 6.27 (br s, PdMe), 8.71 (s, CH_3 of $HNEt_3$), 46.12 (s, CH_2 of $HNEt_3$), 69.09 (br s, CH of fc), 72.69 (br s, CH of fc), 73.97 (d, $^1J_{PC}$ = 56 Hz, C−P of fc), 75.16 (br s, CH of fc), 75.78 (br d, $^2J_{PC}$ = 6 Hz, CH of fc), 94.57 (s, C−SO_3 of fc), 127.91 (d, J_{PC} = 11 Hz, CH of PPh_2), 130.17 (s, CH_{para} of PPh_2), 132.54 (d, $^1J_{PC}$ = 53 Hz, C_{ipso} of PPh_2), 133.85 (d, J_{PC} = 12 Hz, CH of PPh_2). IR (KBr): ν_{max}/cm^{-1} 3431 (br m), 2981 (br w), 2885 (br w), 2686 (br w), 1472 (w), 1432 (m) 1388 (s), 1222 (br, m), 1170 (br s), 1100 (m), 1093 (w), 1037 (s), 835 (w), 742 (w), 691 (m), 654 (s), 543 (w), 494 (m). ESI+ MS: *m*/*z* 571 ([PdMe(**L**) + H]$^+$). Anal. Calcd for $C_{58}H_{74}Cl_2Fe_2N_2O_6P_2Pd_2S_2$·H$_2$O (1434.75): C 48.55, H 5.34, N 1.95%. Found: C 48.71, H 5.10, N 1.94%.

Synthesis of 2. A dichloromethane solution of 4-(dimethylamino)-pyridine (24.4 mg, 0.20 mmol in 5 mL) was added to dimer **1** (143.5 mg, 0.10 mmol) dissolved in the same solvent (3 mL). The mixture was stirred for 3 h and then added onto solid $AgClO_4$ (41.5 mg, 0.20 mmol). After stirring for another 1 h, the mixture was filtered through a PTFE syringe filter (0.45 μm) to remove precipitated AgCl, and the filtrate was washed with water (5× 10 mL) using a separatory funnel. The organic layer was evaporated, leaving an orange residue, which was redissolved in dichloromethane (5 mL), evaporated again, and dried over P_2O_5 under vacuum. The crude product was dissolved in dichloromethane (2 mL) and crystallized by layering with ethyl acetate (8 mL) and hexane (10 mL). A crystalline solid, which separated during several days, was isolated by suction, washed with hexane and pentane, and vacuum-dried. Yield of **2**·0.5CH_2Cl_2·0.5AcOEt: orange crystalline solid, 99.3 mg (64%). ^{1}H NMR (399.95 MHz, $CDCl_3$): δ 0.27 (d, $^3J_{PH}$ = 3.9 Hz, 3 H, PdMe), 3.04 (s, 6 H, NMe_2), 3.98 (vt, J' = 1.9 Hz, 2 H, fc), 4.44 (br vt, J' = 1.9 Hz, 2 H, fc), 4.62 (d vt, J' = 1.9, 0.8 Hz, 2 H, fc), 4.78 (br vq, J' = 2.2 Hz, 2 H, fc), 6.57 (m, 2 H, NC_5H_4), 7.38−7.48 (m, 6 H, PPh_2), 7.58−7.64 (m, 4 H, PPh_2), 8.48 (d, J = 6.4 Hz, 2 H, NC_5H_4). ^{31}P{^{1}H} NMR (161.90 MHz, $CDCl_3$): δ 29.9 (s). ^{13}C{^{1}H} NMR (100.58 MHz, $CDCl_3$): δ 1.75 (d, $^2J_{PC}$ = 5 Hz, PdMe), 39.16 (s, NMe_2), 69.35 (s, CH of fc), 70.53 (s, CH of fc), 72.82 (d, $^3J_{PC}$ = 8 Hz, CH of fc), 73.29 (d, $^1J_{PC}$ = 53 Hz, C−P of fc), 77.17 (d, $^2J_{PC}$ = 13 Hz, CH of fc), 93.32 (s, C−SO_3 of fc), 107.10 (s, CH of NC_5H_4), 128.15 (d, J_{PC} = 11 Hz, CH of PPh_2), 130.40 (d, $^4J_{PC}$ = 2 Hz, CH_{para} of PPh_2), 132.63 (d, $^1J_{PC}$ = 53 Hz, C_{ipso} of PPh_2), 134.06 (d, J_{PC} = 12 Hz, CH of PPh_2), 150.20 (s, CH of NC_5H_4), 154.58 (s, C_{ipso} of NC_5H_4). IR (KBr): ν_{max}/cm^{-1} 3424 (br s), 3077 (w), 2974 (w), 2900 (w), 1616 (vs), 1534 (m), 1435 (m), 1384 (vs), 1251 (s), 1229 (s), 1188 (m), 1155 (m), 1096 (w), 1034 (m), 1019 (m), 842 (m), 812 (m), 746 (m), 694 (m), 639 (m), 525 (w), 499 (m). ESI+ MS: *m*/*z* 571 ([PdMe(**L**) + H]$^+$). Anal. Calcd for $C_{30}H_{31}FeN_2O_3PPdS$·0.5CH_2Cl_2·0.5AcOEt (779.40): C 50.08, H 4.66, N 3.59%. Found: C 50.34, H 4.41, N 3.57%.

Synthesis of 3. Solid Tl[PF_6] (40.9 mg, 0.117 mmol) was added to a solution of **1** (161.1 mg, 0.112 mmol) in anhydrous dichloromethane (10 mL), and the resulting suspension was stirred under a nitrogen atmosphere at room temperature for 1 h. Then, the reaction mixture was filtered through Celite, and the orange filtrate was concentrated to a small volume (3 mL) and precipitated by adding *n*-

DOI: 10.1021/acs.organomet.9b00015
Organometallics XXXX, XXX, XXX−XXX

pentane (15 mL). The orange microcrystalline powder was isolated by suction and dried in a stream of nitrogen. Yield: 134.0 mg (77%). ^{1}H NMR ($CDCl_3$): δ 0.75 (s, 6 H, PdMe), 1.32 (t, $^3J_{HH}$ = 7.3 Hz, 18 H, CH_3 of $HNEt_3$), 3.13 (dq, $^3J_{HH}$ = 7.3 Hz, $^3J_{HH}$ = 5.0 Hz, 12 H, CH_2 of $HNEt_3$), 4.31(br s, 2 H, fc), 4.48 (s, 4 H, fc), 4.70 (br m, 10 H, fc), 7.36−7.59 (m, 20 H, PPh_2), 9.40 (br s, 2 H, *H*NEt_3). ^{31}P{^{1}H} NMR (CDCl): δ 30.7 (s), −144.4 (sept, $^1J_{PF}$ = 704 Hz). ^{13}C{^{1}H} NMR ($CDCl_3$): δ 6.22 (br s, PdMe), 8.81 (s, CH_3 of $HNEt_3$), 46.51 (s, CH_2 of $HNEt_3$), 69.07 (s, CH of fc), 70.70 (br d, $^1J_{PC}$ = 24 Hz, C−P of fc), 72.69−76.40 (m, CH of fc), 94.20 (br s C−SO_3 of fc), 128.15 (br s, CH of PPh_2), 130.58 (s, CH of PPh_2), 131.60 (d, $^1J_{PC}$ = 49 Hz, C^{ipso} of PPh_2), 133.81 (d, J_{PC} = 12 Hz, CH of PPh_2). IR (KBr): ν_{max}/cm^{-1} 3439 (br m), 2996 (br m), 2701 (br m), 1635 (br w), 1472 (m), 1432 (m), 1384 (vs), 1225 (s), 1170 (vs), 1057 (m) 1041 (vs), 838 (vs), 742 (m), 694 (s), 650 (s). Anal. Calcd for $C_{58}H_{74}ClF_6Fe_2N_2O_6P_3Pd_2S_2$ (1526.2): C 45.64, H 4.89, N 1.84%. Found: C 45.15, H 4.70, N 1.83%.

Synthesis of Intermediate ***4***. Complex **1** (100.0 mg, 0.071 mmol) was dissolved in a deaerated, 10:1 (v:v) dichloromethane−acetonitrile mixture (10 mL) to which Tl[PF_6] (50.6 mg, 0.145 mmol) was added under stirring. The reaction mixture was stirred for 2 h and then filtered through a Celite pad to remove separated TlCl. The clear yellow filtrate was washed with deaerated water (2× 10 mL), the organic phase separated, and the solvent evaporated under reduced pressure, thereby forming a yellow powder, which did not dissolve in noncoordinating organic solvents (e.g., chloroform). Yield: 56.5 mg (72%). IR (KBr): ν_{max}/cm^{-1} 3453 (br s), 1635 (br m), 1384 (s), 1225 (w), 1188 (w), 1163 (w), 1100 (w), 1045 (w), 835 (w), 750 (w), 698 (w), 658 (w), 643 (w).

In Situ Synthesis of ***5***. Intermediate **4** (15.0 mg) was dissolved in degassed CD_3CN (0.8 mL) under stirring at room temperature, and the yellow-orange solution was analyzed by NMR spectroscopy. ^{1}H NMR (CD_3CN): δ 0.35 (s, 3 H, PdMe), 4.13 (vt, J = 2.0 Hz, 2 H, fc), 4.42 (vt, J = 1.6 Hz, 2 H, fc), 4.61 (dvt, J = 2.0, 0.7 Hz, 2 H, fc), 4.71 (br m, 2 H, fc), 7.47−7.61 (m, 10 H, PPh_2). ^{31}P{^{1}H} NMR (CD_3CN): δ 31.48 (s). ^{13}C{^{1}H} NMR (CD_3CN): δ − 1.73 (d, $^2J_{PC}$ = 4 Hz, PdMe), 69.56 (s, CH of fc), 70.19 (s, CH of fc), 72.32 (d, $^1J_{PC}$ = 60 Hz, C−P of fc), 73.27 (d, $^3J_{PC}$ = 13 Hz, CH of fc), 77.00 (d, $^2J_{PC}$ = 21 Hz, CH of fc), 94.74 (s, C−SO_3 of fc), 128.43 (d, J_{PC} = 18 Hz, CH of PPh_2), 131.00 (d, J_{PC} = 2 Hz, CH of PPh_2), 131.41 (d, $^1J_{PC}$ = 90 Hz, C_{ipso} of PPh_2), 133.75 (d, J_{PC} = 18.5 Hz, CH of PPh_2). IR (KBr): ν_{max}/cm^{-1} 3453 (br s), 3225 (m), 2981 (w), 2929 (w), 2892 (w), 1660 (s), 1605 (m), 1480 (w), 1432 (m), 1384 (s), 1225 (s), 1188 (s), 1163 (s), 1100 (m), 1045 (s), 835 (m) 750 (m), 698 (m), 658 (s), 643 (m).

Synthesis of ***6***. A solution of (Et_3NH)**L** (220.6 mg, 0.4 mmol) in anhydrous dichloromethane (6 mL) was slowly added to [Pd(μ-Cl)(η^3-C_3H_5)]$_2$ (73.2 mg, 0.2 mmol) dissolved in the same solvent (4 mL). The resulting orange solution was stirred for 3 h and then transferred onto solid $AgClO_4$ (93.2 mg, 0.45 mmol) using 2 × 1 mL of the solvent to rinse the reaction flask. The mixture was stirred for another hour, filtered through a PTFE syringe filter, and then evaporated under vacuum. The residue was taken up with dichloromethane (10 mL) and filtered through a PTFE syringe filter (0.45 μm pore size). The filtrate was layered with dichloromethane−diethyl ether (1:1, 10 mL) and then with diethyl ether (70 mL) in a large test tube. The product is difficult to crystallize, notoriously forming viscous oils. To avoid this problem, the mixture was seeded with a crystal of the product when an orange oil began to separate (the seeding crystal was obtained from a separate experiment performed at a 0.1 mmol scale). The solid, which formed during several weeks, was filtered off, washed with little dichloromethane and diethyl ether, and vacuum-dried. Yield of **6**: 187.0 mg (78%), orange brown solid. ^{1}H NMR (400 MHz, $CDCl_3$): δ 2.70 (s, 1 H, =CH_2 *trans*-O), 2.73 (br s, 1 H, =CH_2 *trans*-O), 4.06 (s, 2 H, fc), 4.22 (dd, J = 9.0, 14.2 Hz, 1 H, =CH_2 *trans*-P), 4.48 (br s, 1 H, fc), 4.54−4.70 (br m, 5 H, fc), 5.21 (t, J = 7.1 Hz, 1 H, =CH_2 *trans*-P), 5.78 (m, 1 H, =CH meso), 7.38−7.55 (br m, 10 H, PPh_2). ^{31}P{^{1}H} NMR (162 MHz, $CDCl_3$): δ 17.9 (s). ^{13}C{^{1}H} NMR (162 MHz, $CDCl_3$): δ 53.55 (d, $^2J_{PC}$ = 2 Hz, =CH_2 *trans*-O), 69.65 (s, CH of fc), 70.14 (s, CH of fc), 72.61 (d, $^1J_{PC}$ = 49 Hz, C−P of fc), 73.22 (br s, CH of fc), 76.12 (br d, J_{PC} = 13 Hz, CH of fc), 85.77 (d, $^2J_{PC}$ = 27 Hz, =CH_2 *trans*-P), 92.56 (s, C−S of fc), 120.01 (d, $^2J_{PC}$ = 5 Hz, =CH meso), 128.66 (d, J_{PC} = 10 Hz, CH of PPh_2), 130.70 (br s, CH of PPh_2), 133.01 (br s, CH of PPh_2), 133.02 (br d, $^1J_{PC}$ = 27 Hz, C_{ipso} of PPh_2). One signal due to ferrocene CH is obscured by the solvent resonance. IR (KBr): ν_{max}/cm^{-1} 3439 (br s), 3070 (w), 1476 (m), 1432 (s), 1384 (vs), 1262 (vs), 1198 (m), 1184 (vs), 1162 (vs), 1158 (vs), 1151 (vs), 1098 (m), 1181 (vs), 1152 (vs), 1096 (m), 1030 (s), 1023 (m), 1004 (m), 930 (w), 831 (m), 827 (m), 748 (m), 744 (m), 698 (s), 658 (s), 639 (s), 617 (vw), 566 (w), 550 (w), 537 (w), 521 (vw), 505 (s), 494 (m), 495 (vs), 466 (s). Anal. Calcd for $C_{25}H_{23}FeO_3PPdS$ (596.71): C 50.32, H 3.88%. Found: C 50.04, H 3.67%.

***Operando* NMR Study with 3.** Compound **3** (10.9 mg, 7 μmol) was dissolved in deaerated $CDCl_3$ (0.9 mL), and the solution was transferred into a 5.0 mm NMR tube under nitrogen. The solution was saturated by slowly bubbling ethylene through the above solution for 5 min, followed by the addition of Na[BAr′$_4$] (12.4 mg, 14 μmol) at room temperature. Then, the NMR tube was sealed and analyzed by ^{31}P{^{1}H} and ^{1}H NMR spectroscopy. The spectra were recorded at room temperature every 15 min. An analogous experiment was carried out also in the presence of pyridine using 2 molar equiv of pyridine with respect to **3**.

***Operando* NMR Study with 7.** In a Schlenk tube, compound **7** (14.4 mg, 13.7 μmol) was dissolved in deaerated $CDCl_3$ (2.0 mL). Then, ethylene was bubbled through the solution at room temperature for a minute, followed by the successive addition of hexadecyltrimethylammonium *p*-toluenesulfonate (12.5 mg, 27.4 μmol) and Na[BAr′4] (24.3 mg, 27.4 μmol) under magnetic stirring. The obtained suspension (NaCl precipitation) was transferred under an ethylene atmosphere into a 5.0 mm NMR tube, which was sealed. ^{1}H and ^{31}P{^{1}H} NMR spectra were acquired at room temperature every half an hour.

Catalytic Experiments. Complex **3** (14.0 mg, 9.0 μmol) was dissolved in deaerated $CDCl_3$ (4.0 mL). Na[BAr′$_4$] (16.0 mg, 18.1 μmol) was added to this solution, and the reaction mixture was stirred for 10 min until NaCl started to precipitate. Then, the suspension was placed in a previously evacuated PTFE-coated stainless-steel autoclave (volume: 70 mL). The autoclave was then pressurized with ethylene to the target pressure, and its content was magnetically stirred for the desired reaction time. Next, the autoclave was cooled to −20 °C, the excess ethylene slowly released, and 0.7 mL of the solution was transferred into a precooled (20 °C) NMR tube. Toluene (25.0 μL, 0.236 mmol) was added as a standard, and ^{1}H NMR spectra were recorded rapidly (20 s) at room temperature.

X-ray Crystallography. Full-sphere diffraction data ($\pm h$ $\pm l$ $\pm l$, completeness ≥99.5%) were collected using a Bruker D8 VENTURE Kappa diffractometer equipped with a Duo PHOTON100 detector, an IμS microfocus source and a Cryostream cooler at 120 or 150 K. The Mo Kα radiation was used throughout.

The structures were solved by direct methods with SHEXLT-2014[32] and refined by full-matrix least-squares against F^2 using SHELXL-2017.[33] All non-hydrogen atoms were refined with anisotropic displacement parameters. The NH hydrogens in the structure of **1**·H_2O were located on the difference electron density map and refined as riding atoms with U_{iso}(H) = 1.2U_{eq}(N). Hydrogen atoms at the π-coordinated allyl ligand in **6** were treated similarly. The remaining hydrogen atoms (in CH_n groups) were included in their theoretical positions and refined as riding atoms with U_{iso}(H) fixed to a multiple of U_{eq} of their bonding carbon atom.

Compound **1**·H_2O crystallized as a nonmerohedral two-component twin (refined contributions = 21:79), and the water molecule in its structure was refined with a fixed geometry (O−H = 0.90 Å). Conversely, compound **2**·1/2AcOEt crystallized as a solvate with one molecule of ethyl acetate molecule per unit cell. The solvent was severely disordered and could not be adequately described. Hence, it was numerically eliminated from the refinement using PLATON SQUEEZE[34] (48 electrons were removed, which ideally matches the expected value).

DOI: 10.1021/acs.organomet.9b00015
Organometallics XXXX, XXX, XXX−XXX

Relevant crystallographic data and structure refinement parameters are presented in the Supporting Information. PLATON[35] was used to prepare all structural drawings and to perform geometric calculations. Numerical values are rounded with respect to their estimated standard deviations (ESDs) given with one decimal place.

DFT Calculations. All the calculations were carried out with Gaussian 09 package[36] using B97D[37] Density functional theory with inclusion of dispersion forces. All optimized structures have been validated as minima or transition states by computed vibrational frequencies. In some cases, relaxed scans were performed to explore the Potential Energy Surface (PES). All calculations were based on the Conductor-like Polarizable Continuum Model (CPCM)[38] for dichloromethane. The effective Stuttgart/Dresden pseudopotential (SDD)[39] was used for Fe and Pd, and the 6-31+G(d,p) basis set with the polarization functions d and p was used for all other atoms. DFT-optimized coordinates are provided in the Supporting Information.

■ ASSOCIATED CONTENT

Supporting Information

The Supporting Information is available free of charge on the ACS Publications website at DOI: 10.1021/acs.organomet.9b00015.

Additional structural diagrams, summary of crystallographic data and structure refinement parameters (Table S1), copies of the NMR spectra, and structural diagrams and energies of the DFT optimized structures (PDF)

Cartesian coordinates of the DFT optimized structures (XYZ)

Accession Codes

CCDC 1889688−1889690 contain the supplementary crystallographic data for this paper. These data can be obtained free of charge via www.ccdc.cam.ac.uk/data_request/cif, or by emailing data_request@ccdc.cam.ac.uk, or by contacting The Cambridge Crystallographic Data Centre, 12 Union Road, Cambridge CB2 1EZ, UK; fax: +44 1223 336033.

■ AUTHOR INFORMATION

Corresponding Authors

*E-mail: petr.stepnicka@natur.cuni.cz (P.Š.).
*E-mail: werner.oberhauser@iccom.cnr.it (W.O.).

ORCID

Werner Oberhauser: 0000-0002-9800-1700
Petr Štěpnička: 0000-0002-5966-0578

Notes

The authors declare no competing financial interest.

■ ACKNOWLEDGMENTS

This work has been supported by Charles University Research Centre program No. UNCE/SCI/014. G.M. acknowledges ISCRA-CINECA HP grants "HP10CFMSCC and HP10C2Q178" and CREA (Centro Richerche Energia e Ambiente) of Colle Val D'Elsa (Siena, Italy) for computational resources.

■ REFERENCES

(1) (a) Nakamura, A.; Anselment, T. M. J.; Claverie, J.; Goodall, B.; Jordan, R. F.; Mecking, S.; Rieger, B.; Sen, A.; van Leeuwen, P. W. N. M.; Nozaki, K. *Ortho*-Phosphinobenzenesulfonate: A Superb Ligand for Palladium-Catalyzed Coordination−Insertion Copolymerization of Polar Vinyl Monomers. *Acc. Chem. Res.* **2013**, *46*, 1438−1449. (b) Nakamura, A.; Ito, S.; Nozaki, K. Coordination−Insertion Copolymerization of Fundamental Polar Monomers. *Chem. Rev.* **2009**, *109*, 5215−5244. (c) Berkefeld, A.; Mecking, S. Coordination Copolymerization of Polar Vinyl Monomers H_2C = CHX. *Angew. Chem., Int. Ed.* **2008**, *47*, 2538−2542.

(2) Selected recent examples: (a) Liang, T.; Chen, C. Side-Arm Control in Phosphine-Sulfonate Palladium- and Nickel-Catalyzed Ethylene Polymerization and Copolymerization. *Organometallics* **2017**, *36*, 2338−2344. (b) Zhang, D.; Chen, C. Influence of Polyethylene Glycol Unit on Palladium- and Nickel-Catalyzed Ethylene Polymerization and Copolymerization. *Angew. Chem., Int. Ed.* **2017**, *56*, 14672−14676. (c) Wang, X.; Nozaki, K. Selective Chain-End Functionalization of Polar Polyethylenes: Orthogonal Reactivity of Carbene and Polar Vinyl Monomers in Their Copolymerization with Ethylene. *J. Am. Chem. Soc.* **2018**, *140*, 15635−15640. (d) Na, Y.; Dai, S.; Chen, C. Direct Synthesis of Polar-Functionalized Linear Low-Density Polyethylene (LLDPE) and Low-Density Polyethylene (LDPE). *Macromolecules* **2018**, *51*, 4040−4048. (e) Liu, Q.; Jordan, R. F. Multinuclear Palladium Olefin Polymerization Catalysts Based on Self-Assembled Zinc Phosphonate Cages. *Organometallics* **2018**, *37*, 4664−4674. (f) Liang, T.; Chen, C. Position Makes the Difference: Electronic Effects in Nickel-Catalyzed Ethylene Polymerizations and Copolymerizations. *Inorg. Chem.* **2018**, *57*, 14913−14919.

(3) (a) Nakano, R.; Chung, L. W.; Watanabe, Y.; Okuno, Y.; Okumura, Y.; Ito, S.; Morokuma, K.; Nozaki, K. Elucidating the Key Role of Phosphine−Sulfonate Ligands in Palladium-Catalyzed Ethylene Polymerization: Effect of Ligand Structure on the Molecular Weight and Linearity of Polyethylene. *ACS Catal.* **2016**, *6*, 6101−6113. (b) Rezabal, E.; Asua, J. M.; Ugalde, J. M. Homopolymerization of Ethylene by Palladium Phosphine Sulfonate Catalysts: The Role of Structural and Environmental Factors. *Organometallics* **2015**, *34*, 373−380. (c) Haras, A.; Anderson, G. D. W.; Michalak, A.; Rieger, B.; Ziegler, T. Computational Insight into Catalytic Control of Poly(ethylene−methyl acrylate) Topology. *Organometallics* **2006**, *25*, 4491−4497.

(4) Noda, S.; Nakamura, A.; Kochi, T.; Chung, L. W.; Morokuma, K.; Nozaki, K. Mechanistic Studies on the Formation of Linear Polyethylene Chain Catalyzed by Palladium Phosphine−Sulfonate Complexes: Experiment and Theoretical Studies. *J. Am. Chem. Soc.* **2009**, *131*, 14088−14100.

(5) Chen, C.; Anselment, T. M. J.; Fröhlich, R.; Rieger, B.; Kehr, G.; Erker, G. *o*-Diarylphosphinoferrocene Sulfonate Palladium Systems for Nonalternating Ethene−Carbon Monoxide Copolymerization. *Organometallics* **2011**, *30*, 5248−5257.

(6) (a) Yang, B.; Pang, W.; Chen, M. Redox Control in Olefin Polymerization Catalysis by Phosphine−Sulfonate Palladium and Nickel Complexes. *Eur. J. Inorg. Chem.* **2017**, *2017*, 2510−2514. (b) Chen, M.; Yang, B.; Chen, C. Redox-Controlled Olefin (Co)Polymerization Catalyzed by Ferrocene-Bridged Phosphine-Sulfonate Palladium Complexes. *Angew. Chem., Int. Ed.* **2015**, *54*, 15520−15524.

(7) Compare the Hammett σ_p constants of − 0.18 and 0.29 for ferrocenyl and its oxidized (ferrocenium) form, respectively: Hansch, C.; Leo, A.; Taft, R. W. A Survey of Hammett Substituent Constants and Resonance and Field Parameters. *Chem. Rev.* **1991**, *91*, 165−195.

(8) (a) Schulz, J.; Císařová, I.; Štěpnička, P. Phosphinoferrocene Amidosulfonates: Synthesis, Palladium Complexes, and Catalytic Use in Pd-Catalyzed Cyanation of Aryl Bromides in an Aqueous Reaction Medium. *Organometallics* **2012**, *31*, 729−738. (b) Schulz, J.; Horký, F.; Císařová, I.; Štěpnička, P. Synthesis, Structural Characterization and Catalytic Evaluation of Anionic Phosphinoferrocene Amidosulfonate Ligands. *Catalysts* **2017**, *7*, 167.

(9) Škoch, K.; Císařová, I.; Štěpnička, P. Synthesis of a Polar Phosphinoferrocene Amidosulfonate Ligand and Its Application in Pd-Catalyzed Cross-Coupling Reactions of Aromatic Boronic Acids and Acyl Chlorides in an Aqueous Medium. *Organometallics* **2016**, *35*, 3378−3387.

(10) Zábranský, M.; Císařová, I.; Štěpnička, P. Synthesis, Coordination, and Catalytic Use of 1′-(Diphenylphosphino)-ferrocene-1-sulfonate Anion. *Organometallics* **2018**, *37*, 1615−1626.

DOI: 10.1021/acs.organomet.9b00015
Organometallics XXXX, XXX, XXX−XXX

(11) Zábranský, M.; Císařová, I.; Trzeciak, A. M.; Alsalahi, W.; Štěpnička, P. Synthesis, Structural Characterization, and Hydroformylation Activity of Rhodium(I) Complexes with a Polar Phosphinoferrocene Sulfonate Ligand. *Organometallics* **2019**, *38*, 479−488.
(12) (a) McGuinness, D. S. Olefin Oligomerization via Metallacycles: Dimerization, Trimerization, Tetramerization, and Beyond. *Chem. Rev.* **2011**, *111*, 2321−2341. (b) Forestiere, A.; Olivier-Bourbigou, H.; Saussine, L. Oligomerization of Monoolefins by Homogeneous Catalysts. *Oil Gas Sci. Technol.* **2009**, *64*, 649−667.
(13) (a) Zheng, F.; Sivaramakrishna, A.; Moss, J. R. Thermal studies on metallacycloalkanes. *Coord. Chem. Rev.* **2007**, *251*, 2056−2071. (b) You, Y.; Girolami, G. S. Mono(cyclopentadienyl)titanium(II) Complexes with Hydride, Alkyl, and Tetrahydroborate Ligands: Synthesis, Crystal Structures, and Ethylene Dimerization and Trimerization Catalysis. *Organometallics* **2008**, *27*, 3172−3180.
(14) (a) Roy, D.; Sunoj, R. B. Ni-, Pd-, or Pt-catalyzed ethylene dimerization: a mechanistic description of the catalytic cycle and the active species. *Org. Biomol. Chem.* **2010**, *8*, 1040−1051. (b) Basu, S.; Arulsamy, N.; Roddick, D. M. Synthesis of $[(dfepe)Pt(Me)(NC_5F_5)]^+B(C_6F_5)_4^-$, a Highly Active Ethylene Dimerization Catalyst. *Organometallics* **2008**, *27*, 3659−3665. (c) Shiotsuki, M.; White, P. S.; Brookhart, M.; Templeton, J. L. Mechanistic Studies of Platinum(II)-Catalyzed Ethylene Dimerization: Determination of Barriers to Migratory Insertion in Diimine Pt(II) Hydrido Ethylene and Ethyl Ethylene Intermediates. *J. Am. Chem. Soc.* **2007**, *129*, 4058−4067. (d) Speiser, F.; Braunstein, P.; Saussine, L. Catalytic Ethylene Dimerization and Oligomerization: Recent Developments with Nickel Complexes Containing P,N-Chelating Ligands. *Acc. Chem. Res.* **2005**, *38*, 784−793.
(15) (a) Kuhn, P.; Sémeril, D.; Matt, D.; Chetcuti, M. J.; Lutz, P. Structure−reactivity relationships in SHOP-type complexes: tunable catalysts for the oligomerisation and polymerisation of ethylene. *Dalton Trans.* **2007**, 515−528. (b) Kim, Y.; Jordan, R. F. Synthesis, Structures, and Ethylene Dimerization Reactivity of Palladium Alkyl Complexes That Contain a Chelating Phosphine−Trifluoroborate Ligand. *Organometallics* **2011**, *30*, 4250−4256. (c) Gott, A. L.; Piers, W. E.; Dutton, J. L.; McDonald, R.; Parvez, M. Dimerization of Ethylene by Palladium Complexes Containing Bidentate Trifluoroborate-Functionalized Phosphine Ligands. *Organometallics* **2011**, *30*, 4236−4249.
(16) Ajellal, N.; Kuhn, M. C. A.; Boff, A. D. G.; Hörner, M.; Thomas, C. M.; Carpentier, J.-F.; Casagrande, O. L., Jr. Nickel Complexes Based on Tridentate Pyrazolyl Ligands for Highly Efficient Dimerization of Ethylene to 1-Butene. *Organometallics* **2006**, *25*, 1213−1216.
(17) Hou, J.; Sun, W.-H.; Zhang, S.; Ma, H.; Deng, Y.; Lu, X. Synthesis and Characterization of Tridentate Nickel Complexes Bearing P∧N∧N and P∧N∧P Ligands and Their Catalytic Property in Ethylene Oligomerization. *Organometallics* **2006**, *25*, 236−244.
(18) Barnard, C. F. J.; Russel, M. H. J. Palladium. In *Comprehensive Coordination Chemistry*; Wilkinson, G., Gillard, R. D., McCleverty, J. A., Eds.; Pergamon Press: Oxford, 1987; Vol. *5*, pp 1099−1130. (b) Hutton, A. T.; Morley, C. P. Palladium(II): Phosphorus Donor Complexes. In *Comprehensive Coordination Chemistry*; G Wilkinson, G., Gillard, R. D., McCleverty, J. A., Eds.; Pergamon Press: Oxford, 1987; Vol. *5*, pp 1157−1170.
(19) Geometric parameters determined for $\mathbf{1}\cdot H_2O$ compare well with those determined for analogous complexes with simple phosphines, *trans*-$[Pd(\mu\text{-}Cl)Me(R_3P\text{-}\kappa P)]_2$, where R = Me and 2-tolyl: Štěpnička, P.; Císařová, I. Formation of Carboxylato-bridged Dipalladium(II) Complexes via Ligand Displacement with a Ferrocene Phosphanocarboxylate. *Z. Anorg. Allg. Chem.* **2004**, *630*, 1321−1325 ref 24b. .
(20) (a) Appleton, T. G.; Clark, H. C.; Manzer, L. E. The trans-influence: its measurement and significance. *Coord. Chem. Rev.* **1973**, *10*, 335−422. (b) Hartley, F. R. *The Chemistry of Platinum and Palladium*; Applied Science: London, 1973; pp 299−303.
(21) Vicente, J.; Arcas, A.; Bautista, D.; Jones, P. G. he Difficulty of Coordinating Mutually *Trans* Phosphine and Aryl Ligands in Palladium Complexes and Its Relation to Important Coupling Processes. Syntheses and Crystal Structures of a Family of Palladium Phosphino, Triflato, Perchlorato, and Aquo-2-(arylazo)aryl Complexes. *Organometallics* **1997**, *16*, 2127−2138.
(22) Piche, L.; Daigle, J.-C.; Poli, R.; Claverie, J. P. Investigation of Steric and Electronic Factors of (Arylsulfonyl)phosphane-Palladium Catalysts in Ethene Polymerization. *Eur. J. Inorg. Chem.* **2010**, *2010*, 4595−4601.
(23) Gan, K.-S.; Hor, T. S. A. 1,1'-Bis(diphenylphosphino)ferrocene — Coordination Chemistry, Organic Syntheses, and Catalysis. In *Ferrocenes*; Togni, A., Hayashi, T., Eds.; Wiley-VCH: Weinheim, 1994; pp 3−104.
(24) (a) Stambuli, J. P.; Incarvito, C. D.; Bühl, M.; Hartwig, J. F. Synthesis, Structure, Theoretical Studies, and Ligand Exchange Reactions of Monomeric, T-Shaped Arylpalladium(II) Halide Complexes with an Additional, Weak Agostic Interaction. *J. Am. Chem. Soc.* **2004**, *126*, 1184−1194. (b) Yamashita, M.; Takamiya, I.; Jin, K.; Nozaki, K. Syntheses and Structures of Bulky Monophosphine-Ligated Methylpalladium Complexes: Application to Homo- and Copolymerization of Norbornene and/or Methoxycarbonylnorbornene. *Organometallics* **2006**, *25*, 4588−4595.
(25) Sreenivasulu, B.; Vetrichelvan, M.; Zhao, F.; Gao, S.; Vittal, J. J. Copper(II) Complexes of Schiff-Base and Reduced Schiff-Base Ligands: Influence of Weakly Coordinating Sulfonate Groups on the Structure and Oxidation of 3,5-DTBC. *Eur. J. Inorg. Chem.* **2005**, *2005*, 4635−4645.
(26) Elschenbroich, C.; Salzer, A. *Organometallics, A Concise Introduction*, 2nd ed.; VCH: Weinheim, 1992; pp 280−287
(27) A similar feature can be found in the structure of $[Pd(\eta^3\text{-}C_3H_5)(2\text{-}Ar_2PC_6H_4SO_3\text{-}\kappa^2O,P)]$ (Ar = 2-methoxyphenyl): Liu, S.; Borkar, S.; Newsham, D.; Yennawar, H.; Sen, A. Synthesis of Palladium Complexes with an Anionic P ∼ O Chelate and Their Use in Copolymerization of Ethene with Functionalized Norbornene Derivatives: Unusual Functionality Tolerance. *Organometallics* **2007**, *26*, 210−216.
(28) Otto, S. Synthesis and crystal structure of a palladium dimer containing ferrocenyldiphenyl-phosphine, *trans*-$[Pd(\mu\text{-}Cl)(CH_3)(PPh_2Fc)]_2$. *J. Chem. Crystallogr.* **2001**, *31*, 185−190.
(29) Rülke, R. E.; Ernsting, J. M.; Spek, A. L.; Elsevier, C. J.; van Leeuwen, P. W. N. M.; Vrieze, K. NMR Study on the Coordination Behavior of Dissymmetric Terdentate Trinitrogen Ligands on Methylpalladium(II) Compounds. *Inorg. Chem.* **1993**, *32*, 5769−5778.
(30) Brookhart, M.; Grant, B.; Volpe, A. F., Jr. $[(3,5\text{-}(CF_3)_2C_6H_3)_4B]^-[H(OEt_2)_2]^+$: A Convenient Reagent for Generation and Stabilization of Cationic, Highly Electrophilic Organometallic Complexes. *Organometallics* **1992**, *11*, 3920−3922.
(31) Silverstein, R. M.; Webster, F. X.; Kiemle, D. J. *Spectrometric Identification of Organic Compounds*; Wiley: Hoboken, NJ, 2005; pp 127−244.
(32) Sheldrick, G. M. *SHELXT*−Integrated space-group and crystal-structure determination. *Acta Crystallogr., Sect. A: Found. Adv.* **2015**, *71*, 3−8.
(33) Sheldrick, G. M. Crystal structure refinement with SHELXL. *Acta Crystallogr., Sect. C: Struct. Chem.* **2015**, *71*, 3−8.
(34) Spek, A. L. *PLATON* SQUEEZE: a tool for the calculation of the disordered solvent contribution to the calculated structure factors. *Acta Crystallogr., Sect. C: Struct. Chem.* **2015**, *71*, 9−18.
(35) Spek, A. L. Structure validation in chemical crystallography. *Acta Crystallogr., Sect. D: Biol. Crystallogr.* **2009**, *65*, 148−155.
(36) Frisch, M. J.; Trucks, G. W.; Schlegel, H. B.; Scuseria, G. E.; Robb, M. A.; Cheeseman, J. R.; Scalmani, G.; Barone, V.; Mennucci, B.; Petersson, G. A.; Nakatsuji, H.; Caricato, M.; Li, X.; Hratchian, H. P.; Izmaylov, A. F.; Bloino, J.; Zheng, G.; Sonnenberg, J. L.; Hada, M.; Ehara, M.; Toyota, K.; Fukuda, R.; Hasegawa, J.; Ishida, M.; Nakajima, T.; Honda, Y.; Kitao, O.; Nakai, H.; Vreven, T.; Montgomery, J. A., Jr.; Peralta, J. E.; Ogliaro, F.; Bearpark, M.;

DOI: 10.1021/acs.organomet.9b00015
Organometallics XXXX, XXX, XXX−XXX

Heyd, J. J.; Brothers, E.; Kudin, K. N.; Staroverov, V. N.; Kobayashi, R.; Normand, J.; Raghavachari, K.; Rendell, A.; Burant, J. C.; Iyengar, S. S.; Tomasi, J.; Cossi, M.; Rega, N.; Millam, J. M.; Klene, M.; Knox, J. E.; Cross, J. B.; Bakken, V.; Adamo, C.; Jaramillo, J.; Gomperts, R.; Stratmann, R. E.; Yazyev, O.; Austin, A. J.; Cammi, R.; Pomelli, C.; Ochterski, J. W.; Martin, R. L.; Morokuma, K.; Zakrzewski, V. G.; Voth, G. A.; Salvador, P.; Dannenberg, J. J.; Dapprich, S.; Daniels, A. D.; Farkas, O.; Foresman, J. B.; Ortiz, J. V.; Cioslowski, J.; Fox, D. J. *Gaussian 09*, revision B.01; Gaussian, Inc.: Wallingford, CT, 2009.

(37) Grimme, S. Semiempirical GGA-type Density Functional Constructed with a Long-range Dispersion Correction. *J. Comput. Chem.* **2006**, *27*, 1787−1799.

(38) (a) Barone, V.; Cossi, M. Quantum Calculation of Molecular Energies and Energy Gradients in Solution by a Conductor Solvent Model. *J. Phys. Chem. A* **1998**, *102*, 1995−2001. (b) Cossi, M.; Rega, N.; Scalmani, G.; Barone, V. Energies, Structures, and Electronic Properties of Molecules in Solution with the C-PCM Solvation Model. *J. Comput. Chem.* **2003**, *24*, 669−681.

(39) Dolg, M.; Stoll, H.; Preuss, H.; Pitzer, R. M. Relativistic and Correlation Effects for Element 105 (Hahnium, Ha): A Comparative Study of M and MO (M = Nb, Ta, Ha) Using Energy-Adjusted Ab Initio Pseudopotentials. *J. Phys. Chem.* **1993**, *97*, 5852−5859.

DOI: 10.1021/acs.organomet.9b00015
Organometallics XXXX, XXX, XXX−XXX